

Comparison of Predicted Forming Limit Curves with Measured Experimental Data on Hot-Dip Zinc-Coated Cold-Rolled Steel by Incremental Forming Process

Ramil Kesvarakul^{1,a*} and Khompee Limpadapun^{2,b}

¹Department of Production Engineering, Faculty of Engineering,
King Mongkut's University of Technology North Bangkok, Thailand

²Department of Industrial Engineering, Faculty of Engineering, Rajapark Institute, Thailand

^aramil.k@eng.kmutnb.ac.th, ^bkhompee.lim@gmail.com

Keywords: Incremental forming process; forming limit curves; deformation mechanism

Abstract. Single Point Incremental Forming (SPIF) is a die-less forming process with advantages of high-flexibility, low-cost and short lead time. The high local strains that are applied to the metal sheet, often exceeding the conventional formability limit. This paper is focused on comparison of predicted forming limit curves with measured experimental data on Hot-Dip Zinc-Coated Cold-Rolled sheet, with 0.20 mm thick is studied in single point incremental forming. Truncated square pyramid and cone are formed to study the formability of blank sheets at room temperature. It was found that both Formulation of plastic instability criteria and Keeler's formula gives the lowest FLC. FLDs have predicted failures in forming process consistently with the real experiments. The experimentally obtained cracking limit differ from analytical one and empirical one by about 3.398 and 2.135 true strain respectively at FLD₀, the corresponding plane strain values.

Introduction

Single Point Incremental Forming (SPIF) is a process for producing complex external shapes and profiles in a sheet metal using a hemispherical shaped tool controlled by means of a CNC milling machine. Since it does not require dies and punch to form a complex shape, it is very appropriate for rapid prototyping. The tool travels in the programmed path and deforms the sheet into desired shape. Some of the outstanding features, such as flexibility, low cost tooling, makes it to be suitable for various applications. It is capable to manufacture various irregular complex components and highly customized medical components [1-3]. The formability of the sheet metal can be predicted by forming limit diagram (FLD) which separates the forming region and failure region. It is represented in terms of major strain and minor strain under plane stress condition [4-6].

In this paper, incremental forming apparatus are developed. Experiment of single point incremental forming with truncated square pyramid and cone are accomplished to study the formability of blank sheets at room temperature. The Experiment result are plotted to FLD and compare with predicted forming limit strains.

Strain-Based Forming Limit Curve

The concept of a forming limit for sheet metal alloys was pioneered by Keeler and Backofen (1963) and Goodwin (1968). They determined experimental forming limits by measuring the principal surface strains on sheet specimens formed to the onset of localized necking. Keeler and Goodwin also generated forming limit diagrams (FLD) in principal strain space in which a forming limit curve (FLC) represents the boundary beyond which there is a risk of necking for a given sheet metal. Therefore, combinations of principal surface strains that place below the FLC lead to a safe forming operation, whereas those that place above it lead to failure.[7]

Formulation of plastic instability criteria Swifts. Swift's diffused necking criterion (Swift, 1952) for thin sheets and Hill's localized necking criterion (Hill, 1952) associated with the Hill's non-

quadratic yield function (Hill, 1979) are used to construct the FLC for the bi-axial tensile strain zone and tensile–compressive strain zone, respectively. The analysis of plastic instability, the following are assumed: (1) The elastic deformation of the material is ignored; (2) The stress state of the tubes is planar; (3) The principal stress ratio at the pole of the forming tube is constant during the bulge tests.

The forming limit curve can be constructed using the obtained critical strain paths ($\varepsilon_1/\varepsilon_2$) for $-0.5 < \xi < 1$. The stress ratio can be obtained as Eq. (1). Calculate Z_d if $\xi \geq 1$ in order to compute subtangent of the stress-strain curve for diffused necking by Eq. (2) and calculate Z_l if $\xi < 0$ in order to compute subtangent of the stress-strain curve for localized necking by Eq. (3). The forming limit for the major and minor principal strain ($\varepsilon_1, \varepsilon_2$) can be obtained by Eq. (4) and (5). The critical major and minor strains are the critical major and minor strains are plotted to construct the forming limit curve (FLC).

$$\alpha = \frac{[(1+2r)|1+\xi|]^{1/(m-1)} - |1-\xi|^{1/(m-1)}}{[(1+2r)|1+\xi|]^{1/(m-1)} + |1-\xi|^{1/(m-1)}} \quad (1)$$

$$Z_d = [2(1+r)]^{1/m} \left\{ \frac{(1+2r)(1-\alpha)|1-\alpha|^{m-1} + (1+\alpha)|1+\alpha|^{m-1}}{(1+\alpha)[(1+2r)^2|1-\alpha|^{2m-2}] + 2(1+2r)(1-\alpha)|1-\alpha^2|^{m-1}} \right\} \quad (2)$$

$$Z_l = \frac{[2(1+r)]^{1/m} [(1+2r)|1-\alpha|^m |1+\alpha|^m]^{(m-1)/m}}{2|1+\alpha|^{m-1}} \quad (3)$$

$$\varepsilon_1 = \frac{2}{[2(1+r)]^{1/m}} \times \frac{nZ}{[|1+\xi|^{m/(m-1)} + (1/1+2r)^{1/(m-1)} |1-\xi|^{m/(m-1)}]^{(m-1)/m}} \quad (4)$$

$$\varepsilon_2 = \varepsilon_1 \xi \quad (5)$$

FLC obtained by Keeler's formula. Empirical FLCs are used to determine the loading paths in this study. The analytical FLCs using the n and r values obtained by tensile tests. The FLC curve approximately according to Keeler's formula as Eq. (6)-(9) and result are shown in Fig. 1.

$$FLD_0 = \frac{n(23.3+14.134t)}{21}, \quad 0 < t < 2.54mm; \quad (6)$$

$$FLD_0 = \frac{n[20+(20.669-1.938t)]}{21}, \quad 2.54 \leq t \leq 5.33mm; \quad (7)$$

$$\varepsilon_{maj} = FLD_0 + \varepsilon_{min}(0.027254\varepsilon_{min} - 1.1965), \quad \varepsilon_{min} > 0; \quad (8)$$

$$\varepsilon_{maj} = FLD_0 + \varepsilon_{min}(-0.008565\varepsilon_{min} - 0.784854), \quad \varepsilon_{min} < 0; \quad (9)$$

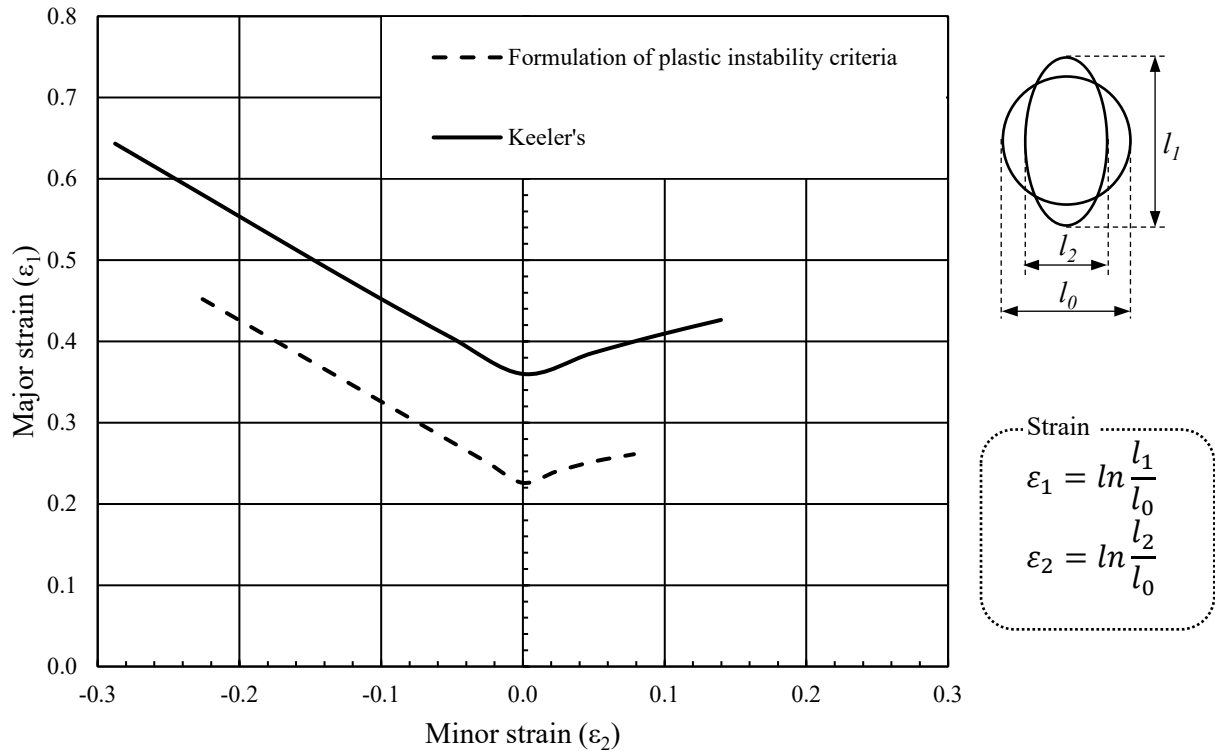


Fig. 1 Forming limit curve from Keeler's formula.

Experimental Setup

Apparatus. In this research, a hemispherical tool of diameter 6 mm. was used to parts. The tool moved along a circular path with increasing steps of depth gradually until reaching the designed depth. The mini numerically controlled router so called mini CNC model LY 3040 was used. The fixture block with the sheet metal mounted on top was installed on the mini CNC machine as shown in Fig. 2.

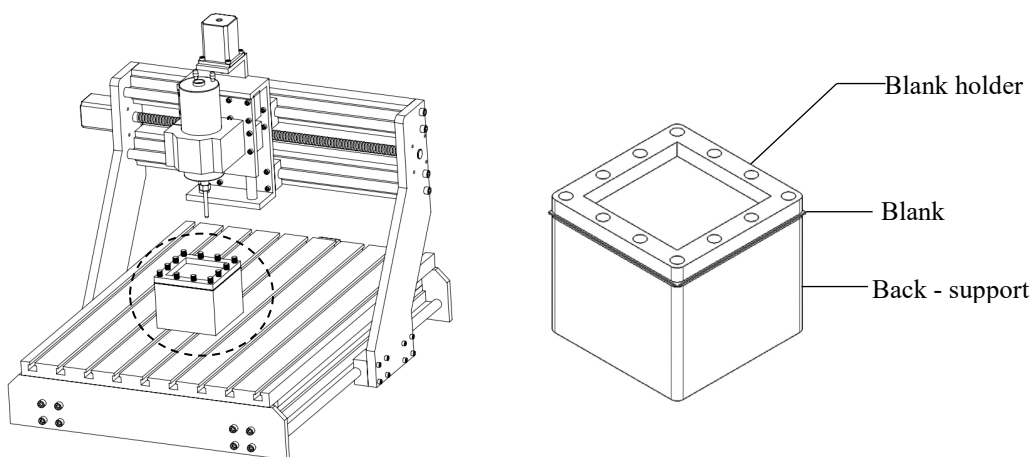


Fig. 2 Fixture for sheet metal camping mounting on CNC Machine.

Specimen. The material in this research was Hot-Dip Zinc-Coated Cold-Rolled sheet, that was produced according to TIS.50-2548. It is commonly used in various application such as sash, shutter door, partition in architecture work, some parts of electric appliances and automobiles.

Specimen for the square sheet blank (104 x 104 mm) by SPIF Is Hot-Dip Zinc-Coated Cold-Rolled sheet blank with 0.20 thickness obtained in cold rolled condition was held into a special design fixture.

The analytical FLC using the n values got from the materials library of Finite Element software. Circular grids were electro chemically etched onto the surface of the metal sheet samples as shown in Fig. 3. The desired pattern stencils then carefully placed on the surface of the metal sheet which in our case was full of the circle grid patterns of 2.5 mm.

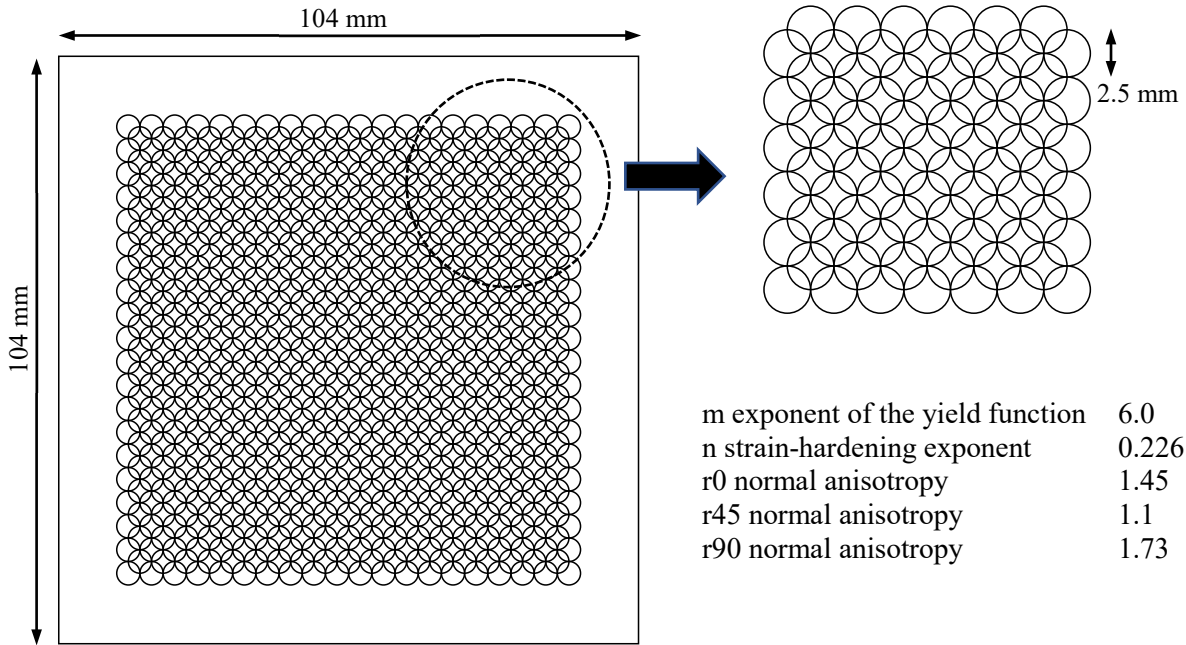


Fig. 3 A specimen with electrochemical grid etched and material property.

The specimen was a truncated square pyramid with 60x60 mm. bottom square and truncated cone with inner diameter at base of 60 mm. with different wall angle ss shown in Fig. 4.

In this research, the specimen was formed by dividing the wall angle to be 3 steps. The wall angle of step-1 and step-2 was constant 45° with 5 mm. in depth and 60° with 5 mm. in depth respectively. For step-3, the wall angle (α) will be changed to various values. The truncated square pyramid will be changed the wall angle from 63° to 65°. The truncated cone will be changed the wall angle from 64° to 65° because the metal sheet will be broken in this range.

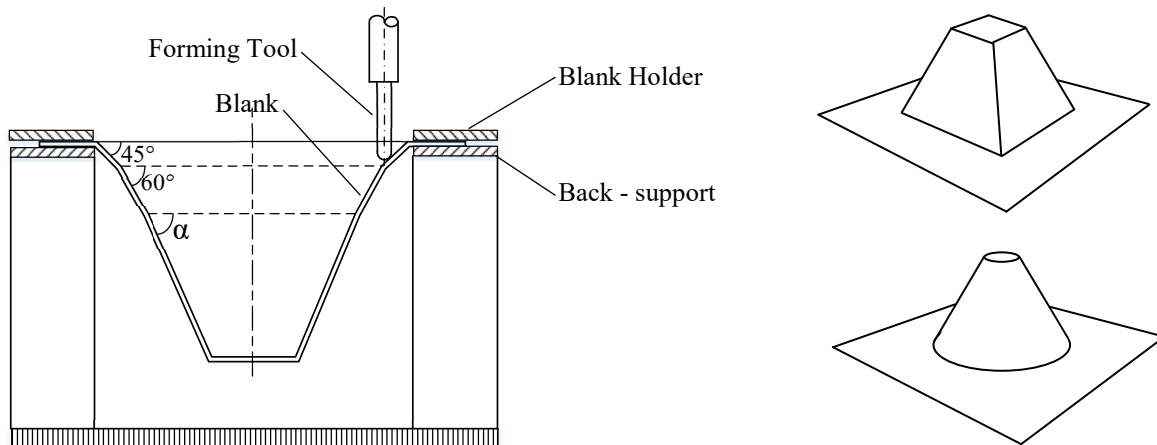


Fig. 4 Truncate square pyramid and cone to be forming.

Forming procedure. The hemispherical tool of diameter 6 mm. was made of stainless steel. The forming tool followed the contour of the desired part with increasing the depth steps until getting the designed depth. The forming parameters were: tool speed 1200 rpm, feed rate 100 mm./min. with increasing steps 0.20 mm in depth and feed rate for moving the tool in the X-Y plane 400 mm./min. The forming tool direction moved along the contour of the desired part in counterclockwise direction as shown in Fig. 5.

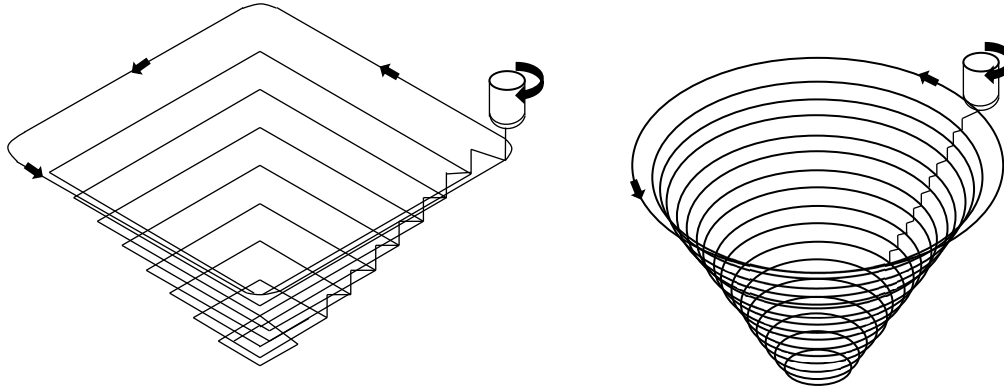


Fig. 5 Tool Path trajectory for truncated square/Cone.

Experimental Procedure. In SPIF, the forming tool with 6 mm. diameter hemispherical head followed the contour of the desired part and imposed a localized plastic deformation. A coconut oil was applied to the blank to reduce friction. It was formed by increasing the depth until it was broken. FLD could be calculated by measuring the deformed circular grids obtained after forming. The researchers started the first research on field using the circular grids which deformed into elliptical after forming. Forming limit diagrams for ISF were obtained by plotting the fracture strain with various test shapes into a Keeler's forming limit diagram.

The circular grids were electro chemically etched onto the surface of the tube samples. After incremental forming tests, the major and minor strains of the grids beside the bursting line on the specimen surface are measured and plotted into the forming limit diagram. Dimensions of the grid circles at the pole were accurately measured to gain the true major and minor strains. The critical major and minor strains were plotted to investigate the cracking point of the forming limit curve (FLC) for sheet material.

Result and Discussion

The formed parts were shown in Fig. 6. In term of formability analysis, circle grid measurement had been used done. This method provides the foundation of predicting in the failure on sheet metal forming. The developing strain can be measured by comparing the circle before and after forming. The circle grids are converted into ellipse during forming. The major and minor strains can be calculated by measuring the lengths of the major and minor stains axes, l_1 and l_2 . The principle strains are calculated by

$$\varepsilon_1 = \ln \frac{l_1}{l_0} \quad (10)$$

$$\varepsilon_2 = \ln \frac{l_2}{l_0} \quad (11)$$

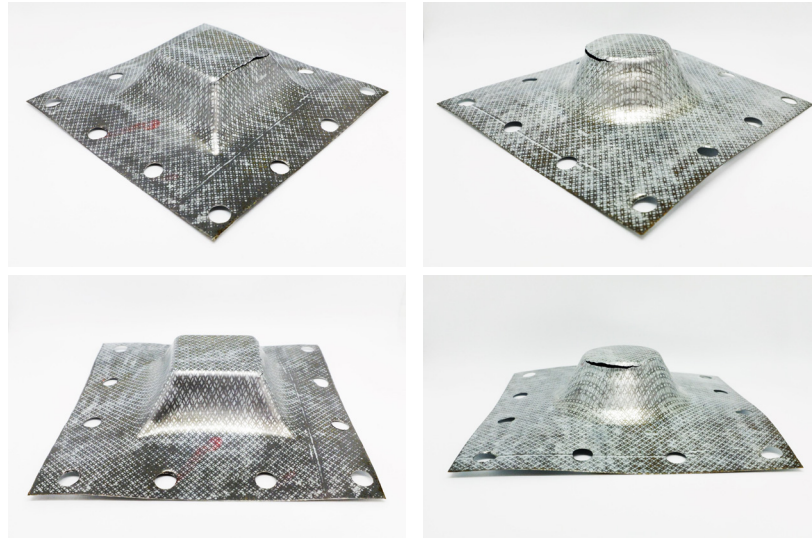


Fig. 6 Formed truncated square pyramid and cone with grid pattern.

FLD graph for ISF was the investigating in the fracture strains plotting against major and minor strains in various shapes shown in Fig. 7. The figure obtained the fracture strains into Keeler's forming limit diagram, formation of plastic instability criteria the truncated square pyramid and cone.

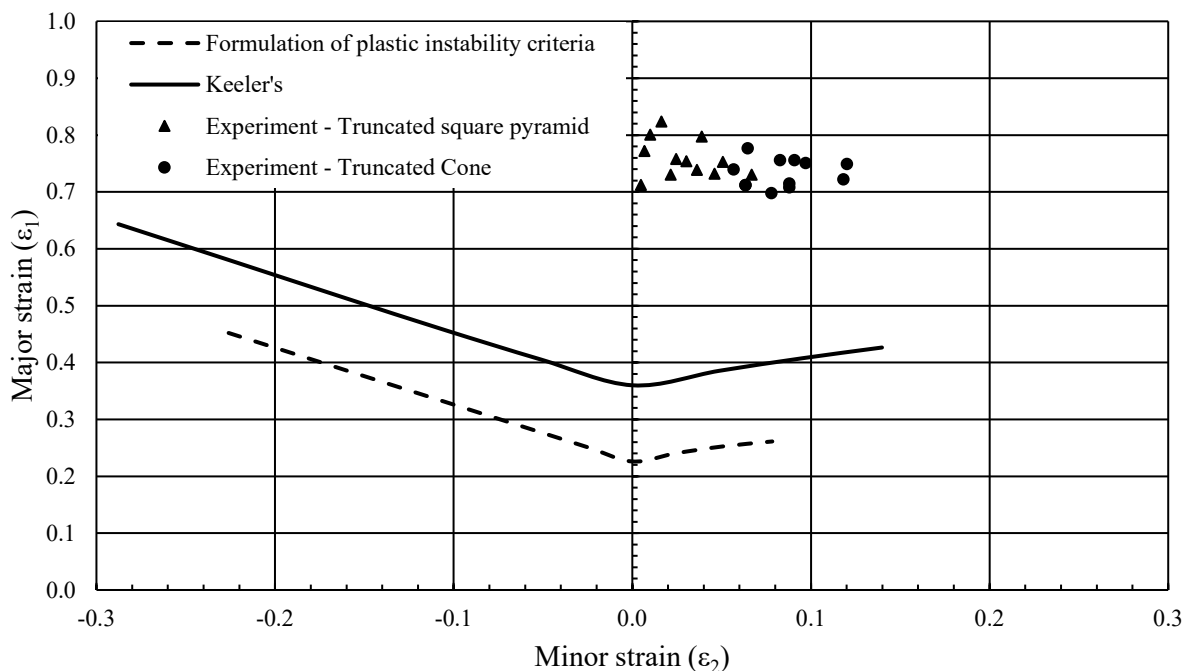


Fig. 7 Comparison of predicted forming limit strains with measured experimental data.

In this research, the forming limit diagram (FLD) was used to describe the formability of materials. The forming Limit Curve (FLC) using for determining the limits of proportional straining before failure was quite difference from the traditional forming. In this case, the slope of the FLC will be negative. The truncated cone had more minor strain than the truncated square pyramid. Regarding to the intersection of Y-axis and trend line of experimental data showed that this method of forming in this material is more than the Keeler's line approximately 2.135 times.

Conclusion

During the forming limit experiments, the loading paths were applied by the single point incremental forming apparatus for Hot-Dip Zinc-Coated Cold-Rolled sheet with 0.20 mm thickness. After forming tests, the major and minor strains of the grids beside the cracking line on the sheet surface were measured to obtain engineering major and minor strains and plotted into the forming limit diagram.

Analytical forming limit curves were also constructed using Swift's diffused and Hill's localized necking criteria associated with Hill's non-quadratic yield function, and Keeler's formula. From the comparison between the analytical and empirical FLCs with the real experimental data, it was found that both formulation of plastic instability criteria and Keeler's formula gave the lowest FLC. FLDs have predicted failures in forming process consistently with the real experiments. The experimentally obtained cracking limit was differed from the analytical one and empirical one (from FEA software) by about 3.398 and 2.135 true strain respectively at FLD_0 , the corresponding plane strain values.

References

- [1] Y.H. Kim, J.J. Park, Effect of process parameters on formability in incremental forming of sheet metal, *Journal of Material Processing Technology*, 130-131 (2002), 42-46.
- [2] J.J. Park, Y.H. Kim, Fundamental studies on the incremental sheet metal forming technique, *Journal of Materials Processing Technology*, 140 (2003), 447– 453.
- [3] G.Ambrogio, L. De Napoli, L.Filice, F.Gagliardi, M.Muzzupappa, Application of incremental forming process for high customized medical product manufacturing, *Journal of Materials Processing Technology*, 204 (2005), 290–303.
- [4] J. Cao, Y. Huang, N.V. Reddy, R. Malhotra, Y. Wang, Incremental sheet forming: Advances and challenges. *Proceedings of International Conference on Technology of Plasticity Kyongju, Korea 2008*.
- [5] M.Subramanian, M.Sakthivel, K.Sooryaprakash, R.Sudhakaran, Optimization of end mill tool geometry parameters for Al7075-T6 machining operations based on vibration amplitude by response surface methodology, *Measurement*, 46 (2013), 4005–4022.
- [6] Amit Kohli, Hari Singh, Optimization of processing parameters in induction hardening using response surface methodology, *Indian Academy of Sciences*, 36 (2011), 141–152.
- [7] Altan, T., & Erman, T. A. , *Sheet Metal Forming Processes and Applications*. Ohio, United State of America: The Materials Information Society.2012